

This paper is published as part of a *CrystEngComm* Collection entitled:

Post-synthetic modification of coordination networks

Guest Editors: Andy Burrows and Seth Cohen

Published in issue 12, 2012 of *CrystEngComm*

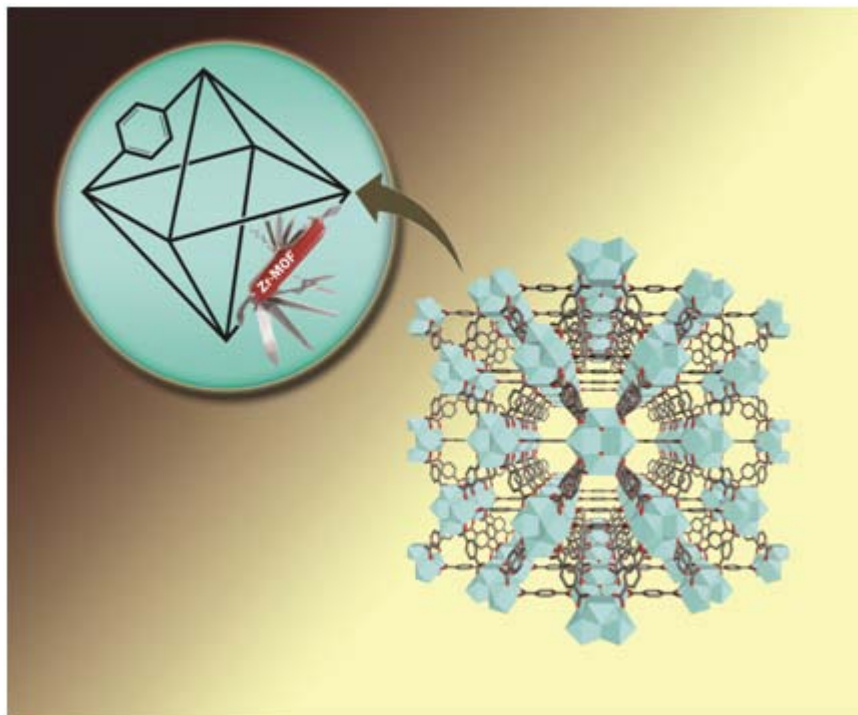


Image reproduced with permission of Seth M Cohen

Articles published in this issue include:

[Discovery, development, and functionalization of Zr\(IV\)-based metal–organic frameworks](#)

Min Kim and Seth M. Cohen

CrystEngComm, 2012, DOI: 10.1039/C2CE06491J

[Controlled modification of the inorganic and organic bricks in an Al-based MOF by direct and post-synthetic synthesis routes](#)

Tim Ahnfeldt, Daniel Gunzelmann, Julia Wack, Jürgen Senker and Norbert Stock

CrystEngComm, 2012, DOI: 10.1039/C2CE06620C

[Conversion of primary amines into secondary amines on a metal–organic framework using a tandem post-synthetic modification](#)

Andrew D. Burrows and Luke L. Keenan

CrystEngComm, 2012, DOI: 10.1039/C2CE25131K

Visit the *CrystEngComm* website for more cutting-edge crystal engineering research
www.rsc.org/crystengcomm

Cite this: *CrystEngComm*, 2012, 14, 4126–4136

www.rsc.org/crystengcomm

PAPER

Controlled modification of the inorganic and organic bricks in an Al-based MOF by direct and post-synthetic synthesis routes†

Tim Ahnfeldt,^a Daniel Gunzelmann,^b Julia Wack,^b Jürgen Senker^{*b} and Norbert Stock^{*a}

Received 2nd December 2011, Accepted 26th January 2012

DOI: 10.1039/c2ce06620c

Four new porous CAU-1 derivatives CAU-1-NH₂ ([Al₄(OH)₂(OCH₃)₄(BDC-NH₂)₃·xH₂O, BDC-NH₂²⁻ = aminoterephthalate), CAU-1-NH₂(OH) ([Al₄(OH)₆(BDC-NH₂)₃·xH₂O), CAU-1-NHCH₃ ([Al₄(OH)₂(OCH₃)₄(BDC-NHCH₃)₃·xH₂O) and CAU-1-NHCOCH₃ ([Al₄(OH)₂(OCH₃)₄(BDC-NHCOCH₃)₃·xH₂O) all containing an octameric [Al₈(OH)_{4+y}(OCH₃)_{8-y}]¹²⁺ cluster, with *y* = 0–8, have been obtained by MW-assisted synthesis and post-synthetic modification. The inorganic as well as the organic unit can be modified. Heteronuclear ¹H–¹⁵N, ¹H–¹³C and homonuclear ¹H–¹H connectivities determined by solid-state NMR spectroscopy prove the methylation of the NH₂ groups when conventional heating is used. Varying reaction times and temperatures allow controlling the degree of methylation of the amino groups. Short reaction times lead to non-methylated CAU-1 (CAU-1-NH₂), while longer reaction times result in CAU-1-NHCH₃. CAU-1-NH₂ can be modified chemically by using acetic anhydride, and the acetamide derivative CAU-1-NHCOCH₃ is obtained. Thermal treatment permits us to change the composition of the Al-containing unit. Methoxy groups are gradually exchanged by hydroxy groups at 190 °C in air. Solid-state NMR spectra unequivocally demonstrate the presence of the amino groups, as well as the successful post-synthetic modification. Furthermore ¹H–¹H correlation spectra using homonuclear decoupling allow the orientation of the NHCOCH₃ groups within the pores to be unravelled. The influence of time and temperature on the synthesis of CAU-1 was studied by X-ray powder diffraction, elemental analyses, and ¹H liquid-state NMR and IR spectroscopy.

1. Introduction

Metal–organic frameworks (MOFs) have evolved over the past decade into the most investigated class of porous materials.¹ Based on their high thermal stability, well defined pore systems and high porosity, some MOFs are suitable for a number of potential applications, such as controlled drug release,² storage and separation of gases,³ as catalysts⁴ and in sensing devices.⁵ For most of the applications very low framework density and/or additional functional groups in the pores are required. To achieve a low framework density, MOFs which are based on light metals such as magnesium or aluminium are promising.⁶ In the last decade aluminium-containing MOFs (Al-MOFs) have been investigated intensively.⁷ Al-based MOFs are known for

their high thermal and chemical stability, non-toxicity and large apparent specific BET surface areas.⁸ Al-MOFs can be synthesised using common linker molecules, such as terephthalic acid,⁹ naphthalenedicarboxylic acid¹⁰ and trimesic acid.¹¹ Starting from the terephthalic acid linker additional functional groups, like hydroxy-, nitro-, chloro-, bromo-, and methyl-groups, were successfully incorporated into Al-MOFs *via* isoreticular synthesis strategies.¹² The modified frameworks show often different sorption¹³ and improved catalytic properties,¹⁴ which are based on different host–guest interactions. The most common functional group in Al-MOFs is the amino group. The amino group is chemically inert in most solvents and does not participate in the coordination chemistry of the metal ions. Furthermore, the amino group allows post-synthetic modification reactions on the pore surfaces such as nucleophilic substitution, acid–base reactions or condensation reactions.¹⁵ Modified linker molecules can change properties like the accessibility of the pores and thus sorption behaviour depending on their orientation within the pores. The orientation of linker residues, however, is difficult to determine and mostly unknown. Solid-state NMR spectroscopy is a powerful tool for this task. It enables the determination of distances, angles and orientation correlations. Based on the aminoterephthalic acid linker the amino group could be successfully incorporated into the

^aInstitut für Anorganische Chemie Christian-Albrechts-Universität, Max-Eyth Strasse 2, 24118 Kiel, Germany. E-mail: stock@ac.uni-kiel.de; Fax: +49 4318801775; Tel: +49 4318801675

^bAnorganische Chemie III, Universität Bayreuth, Universitätsstraße 30, 95447 Bayreuth, Germany. E-mail: juergen.senker@uni-bayreuth.de; Tel: +49 921552532

† Electronic supplementary information (ESI) available: Additional results of solid state and solution-based NMR spectroscopic studies, X-ray powder diffraction and temperature dependent X-ray powder diffraction patterns and results of the thermogravimetric measurements. See DOI: 10.1039/c2ce06620c

structures of MIL-53 (ref. 16) and MIL-101.^{17,18} Very recently we synthesised CAU-1 using the aminoterephthalic acid linker.¹⁷ The CAU-1 framework¹⁹ contains $[\text{Al}_8(\text{OH})_4(\text{OCH}_3)_8]^{12+}$ clusters composed of eight distorted AlO_6 -octahedra that are connected through hydroxy groups (corner-sharing) and two methoxy groups (edge-sharing). The arrangement of these clusters can be derived from a tetragonally distorted bcc arrangement. These clusters are twelve-fold connected *via* amino terephthalate ions. The structure possesses two kinds of cavities with effective diameters of approximately 1 and 0.45 nm. Twelvefold connected networks, such as UiO-66 (ref. 20) and MIL-125,²¹ are known for their stability and high porosity. CAU-1 has been intensively investigated, for example in the field of thin-film crystal growth,²² N_2 , H_2 , and CO_2 -sorption^{23,24} and post-synthetic modification,²⁵ and its formation has been studied by *in situ* EDXRD measurements.^{12a,26} The first publication on CAU-1 (ref. 17) depicts a signal at ~ 27 ppm in the ^{13}C CP MAS solid-state NMR spectrum, which could not be assigned at that time. This prompted us to carry out an in-depth investigation which also revealed the origin of the ^{13}C signal. Herein we show that the signal is due to the methylation of the amino group. We also demonstrate the influence of the reaction time and temperature on the *in situ* methylation of CAU-1-NH₂. In addition, the post-synthesis modification by reaction with acetic anhydride is shown and the influence of thermal activation on the composition of the Al-based building unit is identified.

2. Experimental

2.1 Chemicals

$\text{AlCl}_3 \cdot 6\text{H}_2\text{O}$ (Riedel-de Haen, $\geq 99\%$), $\text{H}_2\text{BDC-NH}_2$ (Fluka, $\geq 98\%$), methanol (BASF, purum), and acetic anhydride (Fluka, $\geq 99\%$).

2.2 Methods

X-Ray powder diffraction patterns were recorded with a STOE STADI P diffractometer equipped with a linear position sensitive detector using monochromatic $\text{Cu-K}_{\alpha 1}$ radiation. Lattice parameters were determined using the DICVOL²⁷ program and refined using the STOE software package WinXPow.²⁸ Temperature-dependent X-ray powder diffraction (TD-XRPD) experiments were performed under air with a STOE STADI P diffractometer equipped with an image plate detector and a STOE capillary furnace (version 0.65.1) using monochromatic $\text{Cu-K}_{\alpha 1}$ radiation. Each powder pattern was recorded in the $4\text{--}35^\circ$ range (2θ) at intervals of 10°C up to 350°C and intervals of 25°C from $350\text{--}400^\circ\text{C}$ with duration of 15 min per scan. The temperature ramp between two patterns was set to 2°C min^{-1} .

Thermogravimetric (TG) analysis was carried out in air (75 mL min^{-1} , $25\text{--}900^\circ\text{C}$, 4°C min^{-1}) on a Netzsch STA-409CD. Carbon, hydrogen, and nitrogen contents were determined by elemental chemical analysis on an Eurovektor EuroEA Elemental Analyzer. EDX analysis was performed on a Philips ESEM XL 30. IR spectra were recorded on an ATI Matheson Genesis in the spectral range $4000\text{--}400\text{ cm}^{-1}$ using the KBr disk method as well as on an ALPHA-ST-IR Bruker spectrometer equipped with an ATR unit.

Several types of adsorption experiments were carried out using three different gases. Based on the TG data, activation at 130°C under vacuum for 3 h was used for all measurements. The specific surface area of the dehydrated CAU-1 derivatives was determined by measuring the N_2 sorption isotherms at -196°C using a BELSORP-max apparatus. Approximately 30 mg of sample were used for each experiment. The CO_2 and H_2O adsorption experiments were carried out at 25°C up to a pressure of 1 bar using the same instrument.

For the NMR study of the CAU-1 samples liquid- and solid-state NMR experiments were performed. Liquid-state NMR spectra were recorded on a Bruker DRX500 operating at 500 MHz for ^1H . Two different procedures were applied to obtain solution samples for the liquid-state NMR investigations. In the first method, the washed CAU-1 material was directly dissolved in a dilute $\text{NaOD/D}_2\text{O}$ solution. In the second method the linker was isolated by digesting the framework in 2 M NaOH and reprecipitating by neutralising using 2 M HCl. After filtration, the linker was redissolved in a dilute $\text{NaOD/D}_2\text{O}$ solution.

The 1D solid-state NMR experiments were carried out on commercial BRUKER Avance DSX-300 and Avance II 300 spectrometers operating at 7.05 T with resonance frequencies of 75.47 MHz for carbon and of 30.41 MHz for nitrogen. 2D experiments were measured on a BRUKER Avance III 400 spectrometer operating at 9.4 T with resonance frequencies for ^1H and ^{13}C of 400.13 MHz and 100.62 MHz. The proton and carbon shifts were referenced relative to tetramethylsilane and the nitrogen shifts to nitromethane. The carbon–proton 2D MAS-J-HMQC²⁹ experiment of solvothermally synthesised CAU-1 was performed using a 4 mm double-resonance probe with the sample restricted to the inner third of the rotor to increase rf field homogeneity and spinning at 10 kHz rotation frequency. The contact time for the cross-polarisation was set to 5 ms and the delay τ equal to 2 ms. The proton rf field strength was set to 83 kHz during τ (FSLG decoupling) and 100 kHz during acquisition (Spinal64 decoupling). All proton–proton homonuclear and carbon–proton heteronuclear correlation experiments were measured accordingly at 12.5 kHz rotation frequency with a ^1H nutation frequency of 76 kHz for excitation and decoupling (using the eDUMBO sequence during t_1 and the windowed wDUMBO sequence during t_2). The 1D ^{13}C and ^{15}N CPMAS spectra were collected in 4 mm or 7 mm triple resonance probes with spinning speeds between 5 and 8 kHz. These spectra were recorded using a cross-polarization sequence with a nutation frequency of the protons of 77 kHz (sweeping from 50 to 100% power) and a Spinal64 proton decoupling of 63 kHz for the ^{13}C spectra and 89 kHz proton nutation frequency and spinal64 proton decoupling of 71 kHz for the ^{15}N spectra. The relaxation times were checked and the recycle delays set accordingly to 5 s for CAU-1-NH₂, 2.5 s for CAU-1-NHCOCH₃ and 2.5 s for CAU-1-NHCH₃, respectively.

For the microwave reactions the commercially available microwave synthesizer Biotage Initiator was used. The reaction temperature attained within 1 min corresponds to ramp rates of $2\text{--}5^\circ\text{C s}^{-1}$. Glass reactor vials (Biotage microwave vial 2–5 mL) with an inner diameter of 14 mm and a volume of 10 mL were used. Temperatures were measured by an internal IR sensor.

Conventional syntheses were carried out in glass reactors (DURAN® glass 25 mL) and Teflon-lined steel autoclaves with a maximum volume of 30 mL.

2.3 Systematic investigation of the influence of reaction time and temperature on the methylation of CAU-1

Based on previous results obtained from the *in situ* EDXRD crystallisation studies the reactions were carried out in a microwave (MW) oven (Biotage Initiator) using 5 mL glass vials.^{12a,26} For all reactions a mixture of $\text{AlCl}_3 \cdot 6\text{H}_2\text{O}$ (232 mg, 0.961 mmol) and $\text{H}_2\text{BDC-NH}_2$ (58 mg, 0.312 mmol) was used, which was suspended in methanol (3.175 mL). The influence of reaction time was studied at 135 °C in a time range of 15–638 min and at 145 °C between 2 and 10 min.

2.4 Synthesis of CAU-1-NH₂, [Al₄(OH)₂(OCH₃)₄(BDC-NH₂)₃]

The non-methylated compound CAU-1-NH₂ was synthesised using MW-assisted heating. A mixture of $\text{AlCl}_3 \cdot 6\text{H}_2\text{O}$ (232 mg, 0.961 mmol) and $\text{H}_2\text{BDC-NH}_2$ (58 mg, 0.312 mmol) was suspended in methanol (3.175 mL) in a 5 mL glass vial. After sealing, the reaction mixture was heated under stirring (300 r s⁻¹) at 145 °C for 3 min. The reaction mixture was rapidly cooled to room temperature. A yellow microcrystalline dispersion was obtained. After centrifugation, the product was redispersed in water (25 mL) to remove the Cl⁻ ions, which may be present due to the formation of R-NH₃⁺ groups. This procedure was repeated (three times) until no Cl⁻ ions could be detected anymore. The final product was dried in air to yield CAU-1-NH₂ (75% for the as-synthesised product and 50% for the activated compound based on aminoterephthalic acid). Elemental analysis of the washed phase: observed, C: 41.22, H: 3.65, N: 5.46; calculated (based on [Al₄(OH)₂(OCH₃)₄(BDC-NH₂)₃]), C: 41.84, H: 3.64, N: 5.22%.

2.5 Synthesis of CAU-1-NHCH₃, [Al₄(OH)₂(OCH₃)₄(BDC-NHCH₃)₃]

The methylated compound was synthesised using MW-assisted heating by increasing the reaction time. A mixture of $\text{AlCl}_3 \cdot 6\text{H}_2\text{O}$ (232 mg, 0.961 mmol) and $\text{H}_2\text{BDC-NH}_2$ (58 mg, 0.312 mmol) was suspended in methanol (3.175 mL) and heated to 135 °C for 10 h. A yellow microcrystalline product was obtained after filtering and drying in air. Like CAU-1-NH₂, the as-synthesised products contain large amounts of Cl⁻ ions. To remove these, the raw product was washed several times with water to yield CAU-1-NHCH₃. Elemental analysis of the washed phase: observed, C: 44.03, H: 4.18, N: 4.97; calculated (based on [Al₄(OH)₂(OCH₃)₄(BDC-NHCH₃)₃]), C: 43.31, H: 4.10, N: 4.98%.

2.6 Post-synthetic modification of CAU-1-NH₂

To [Al₄(OH)₂(OCH₃)₄(BDC-NH₂)₃] (500 mg, 0.626 mmol) acetic anhydride (2 mL, 21.197 mmol) was added. The reaction was carried out in an ultrasonic bath (160 W Bandelin Sonorex RK 100) at room temperature for 3 h leading to the formation of the amide derivative. The product was washed with H₂O and heated in air (80 °C, 2 h) to yield CAU-1-NHCOCH₃. Elemental analysis: observed, C: 35.59, H: 3.50, N: 3.63; calculated (based

on [Al₄(OH)₂(OCH₃)₄(BDC-NHCOCH₃)₃·xH₂O; x ≈ 12) C: 35.68, H: 3.59, N: 3.67%.

2.7 Thermal activation of CAU-1-NH₂

To remove solvent molecules from the pores of CAU-1-NH₂, the samples were treated thermally. Depending on the activation conditions (vacuum vs. air) and the applied temperatures (120–190 °C), a substitution of methoxy groups by hydroxy groups in the Al-based brick of the CAU-1-NH₂ framework takes place. At an activation temperature of 190 °C the methoxy groups were fully replaced by hydroxy groups after 24 h and CAU-1-NH₂(OH) ([Al₄(OH)₆(BDC-NH₂)₃·xH₂O) is formed.

3. Results and discussion

3.1 Solid-state NMR investigation of CAU-1 synthesised under conventional heating

The unassigned carbon signal at 27 ppm (see Ahnfeldt *et al.*,¹⁷ Fig. S5b†) gave rise to the question whether the product is phase pure. By performing a carbon–proton 2D MAS-J-HMQC experiment the carbon signals are correlated to signals of directly bonded hydrogen nuclei. In the HMQC spectrum (Fig. 1) the signal at 27 ppm correlates with a proton signal at 2.2 ppm, characteristic of a methyl group, the signal at 57 ppm with the methoxy proton signal at 2.8 ppm, and the directly proton bonded aromatic carbons (113, 116, and 132 ppm) correlate with proton signals between 7 and 8 ppm. Non-bonded carbons, like the carboxy (174 ppm) or the quaternary aromatic carbons (153, 137 and 115 ppm), show no correlation to protons in this experiment, but can be seen in the top of Fig. 1 for comparison.

The same proton signals were found in proton–proton homonuclear correlation (HOMCOR) spectra (Fig. 2 and S1†) as well as in carbon–proton heteronuclear (HETCOR) spectra (shown in Fig. S2†). All these 2D spectra exhibit cross-peaks

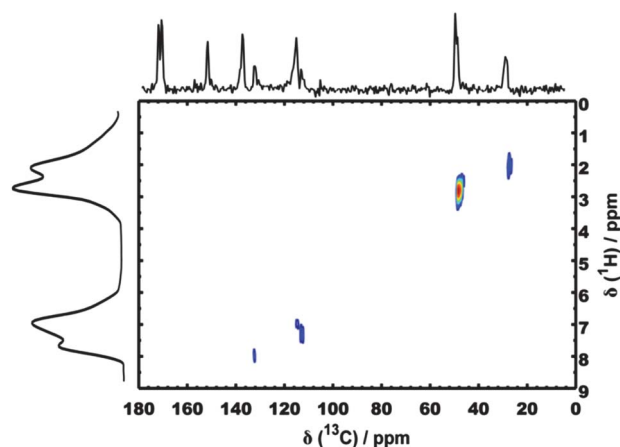


Fig. 1 ¹H-¹³C-MAS-J-HMQC spectrum of CAU-1 synthesised under conventional heating showing correlations between directly bonded protons to carbon nuclei. For comparison a ¹³C CP spectrum of the sample, depicting all carbon signals, is shown on top. On the left the homonuclear decoupled ¹H spectrum is shown.

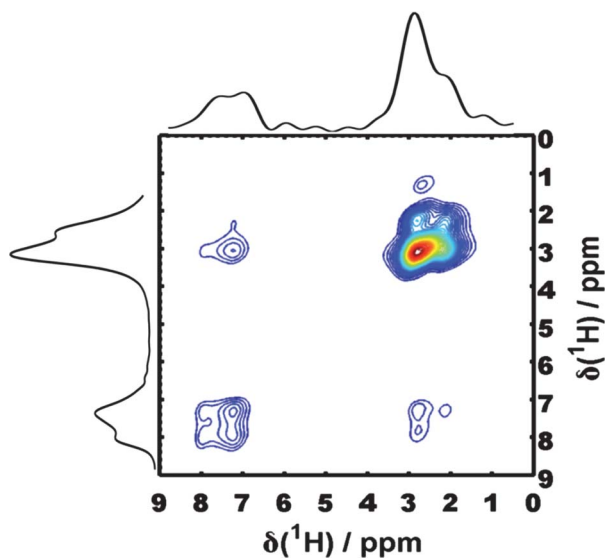


Fig. 2 ^1H - ^1H HOMCOR spectrum of conventionally synthesized CAU-1 with DUMBO decoupling during t_1 and t_2 and a spin diffusion time of 4 ms, showing also longer proton-proton distance correlations.

between either the ^1H signal at 2.2 ppm or the ^{13}C signal at 27 ppm and other characteristic resonances. For example in Fig. 2 the ^1H signal at 2.2 ppm couples with the resonances in the aromatic region. These experiments therefore allow the assignment of a methyl group as an integral part of the CAU-1 structure. A final clue to its nature is given by the ^{15}N -CPPI experiment (Fig. 3) that shows different nitrogen signals.

The intensity modulation due to a CPPI sequence (Fig. 3, inset) reveals that the ^{15}N resonances at -319 and -323 ppm bear $-\text{NH}$ functionalities while the one at -347 ppm seems to be a tertiary N atom. Together with the shift values the signals at -319 and -323 ppm can be assigned to $-\text{NHCH}_3$ groups while the one at -347 ppm is probably a $-\text{N}(\text{CH}_3)_2$ group. By the HMQC experiment we could prove the methyl group to be an integral part of the structure and *via* the CPPI experiment we could prove the methylation of the amino group. The CAU-1 synthesised under conventional heating therefore is methylated

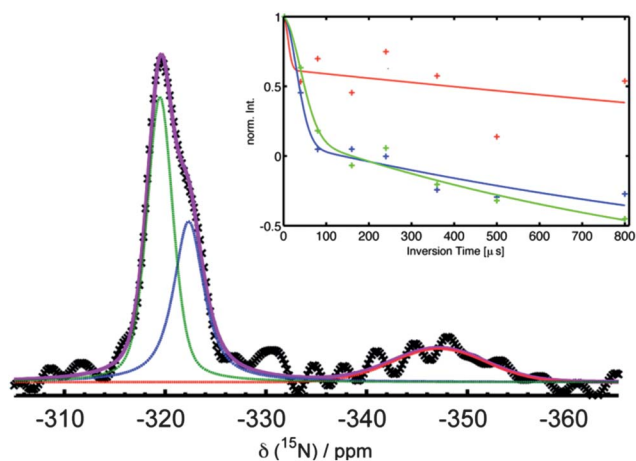


Fig. 3 ^{15}N -CPPI-spectrum and intensity decrease (shown in the inset) for the signals at -319 (green), -323 (blue) and -347 ppm (red).

at the aminoterephthalic linker molecules. It is worth noting that the occurrence of two different shifts for the NHCH_3 groups indicates two different scenarios for the orientation of the functional groups within the pores with one alignment being more probable by a factor of 2. Parameters influencing this methylation reaction are studied in the following.

3.2 Influence of the reaction temperature

The synthesis of CAU-1 under MW-assisted heating was carried out in the temperature range 115 – 145 °C. The reaction time for each temperature was determined from the *in situ* EDXRD studies on CAU-1 (ref. 26) and corresponds to the time required to reach full crystallisation (ranging from 105 min for 115 °C to 7–9 min for 145 °C, Table S1†). The reaction products were filtered and washed once with water. The XRPD patterns of the reaction products are shown in Fig. S3† and demonstrate that CAU-1 was formed at all reaction temperatures. The corresponding IR spectra of the reaction products are shown in Fig. 4.

The IR spectra of CAU-1 show the characteristic bands for the symmetric and asymmetric stretching modes of the bridging carboxylate group between 1600 and 1400 cm^{-1} . The presence of methoxy groups in the structure of CAU-1 is clearly demonstrated by the asymmetric and symmetric C–H stretching vibrations at 2940 and 2835 cm^{-1} as well as the C–O stretching vibration at ~ 1080 cm^{-1} . The typical bands for the NH_2 group at ~ 3500 and 3380 cm^{-1} (symmetric and asymmetric N–H vibrations) are not observed, because they are obscured by a broad intensive band between 3200 and 3600 cm^{-1} due to the presence of water molecules. The characteristic double band for the $\text{C}_{\text{ar}}-\text{N}(\text{NH}_2)$ (ar = aromatic) vibration at 1254 and 1334 cm^{-1} can be observed in all spectra.³⁰ The relatively high intensities of these characteristic amino-bands indicate a large quantity of non-methylated NH_2 groups. This suggests that the reaction temperature has no or only minor influence on the methylation of CAU-1.

3.3 Influence of the reaction time on the degree of methylation at the reaction temperature of 135 °C

To study the influence of the reaction time on the degree of methylation, five reactions were carried out under MW-assisted

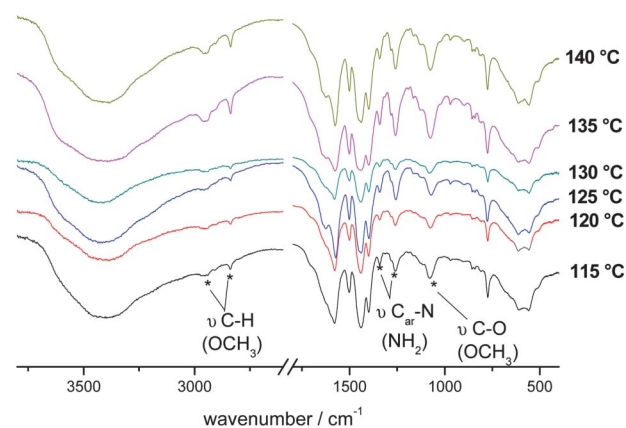


Fig. 4 IR-spectra of the CAU-1 product obtained by MW-assisted heating carried out in the temperature range between 115 and 140 °C.

heating at 135 °C. Reaction times were varied between 15 min and 638 min. The reaction products were characterized by elemental analyses, IR-spectroscopy and ^1H liquid-state NMR spectroscopy, which is the most powerful of the three methods. Employing ^1H NMR spectroscopy the digested reaction products, which contain only the isolated linker molecules redissolved in a dilute NaOD/D $_2\text{O}$ solution, were characterised (Fig. 5). Elemental analyses and IR-spectroscopy were performed on the activated products. Two sets of signals are observed in the ^1H NMR spectra which belong to aminoterephthalate and *N*-methylaminoterephthalate ions. The sets of ^1H signals are labelled as follows (Scheme 1). The intensity of the resonance corresponding to the protons of the methyl group from the BDC-NHCH $_3^{2-}$ ions at 2.22 ppm in the ^1H NMR spectra (Fig. 5) increases with increasing reaction time due to the methylation of the amino groups. The degree of methylation was calculated from the sum of integrals of the aromatic H atoms and the integral of the methyl groups. This procedure is applied to all spectra that are discussed in this study.

The degree of methylation depends strongly on the reaction time. After a reaction time of 15 min only 8% of the amino groups are methylated. This value increases to 47 and 95% after a reaction time of 98 and 638 min, respectively. Furthermore small signals at 2.17 and 2.13 ppm appear in the spectra after a reaction time above 38 min, which indicates some multiple methylation of the amino groups at longer reaction times. Thus, post-synthetic modification, *i.e.* methylation, of CAU-1-NH $_2$ takes place within the cages. This reaction could be catalysed by Lewis acidic sites of free Al $^{3+}$ ions in the reaction solution.

Focusing on the 6.0–7.3 ppm range the two sets of signals due to the methylated and non-methylated product are clearly distinguishable. Thus the degree of methylation is also visible in the aromatic ^1H region. In comparison to CAU-1-NH $_2$ the ^1H signals of the aromatic H atoms of CAU-1-NHCH $_3$ (labelled red) are shifted by about ± 0.04 ppm (Fig. 5, left).

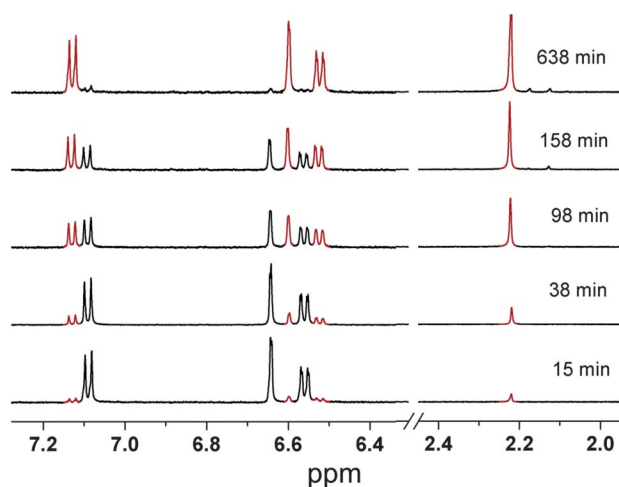
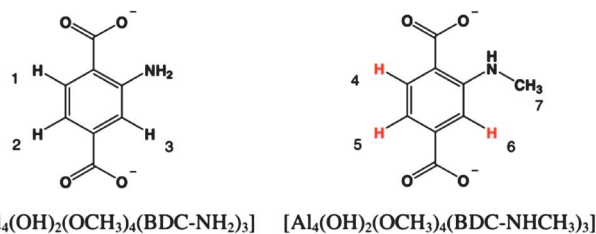


Fig. 5 ^1H NMR spectra of the extracted aminoterephthalate linkers collected from the MW-assisted syntheses at 135 °C using reaction times between 15 and 638 min. Each spectrum is normalized to the sum of the aromatic H signals (methylated (black) and non-methylated (red)), the aromatic signals (left) are multiplied by 2.5 relative to the methyl signals (right) for better visualisation.



Scheme 1 Labelling of the ^1H signals in methylated and non-methylated aminoterephthalate ions: ^1H NMR 500 MHz, (NaOD/D $_2\text{O}$) δ : BDC-NH $_2^{2-}$: 7.09 (d, 1H, H1 $^3J_{\text{H-H}} = 8.1$ Hz); 6.64 (s, 1H, H3); 6.56 (d, 1H, H2 $^3J_{\text{H-H}} = 8.1$ Hz); BDC-NHCH $_3^{2-}$: 7.13 (d, 1H, H4 $^3J_{\text{H-H}} = 8.0$ Hz); 6.60 (s, 1H, H6); 6.52 (d, 1H, H5 $^3J_{\text{H-H}} = 8.0$ Hz); 2.22 (s, 3H, H7).

The methylation of the amino group leads to a low field shift for the protons in the *meta*-position (H4) and to a high field shift for the protons in *ortho*- and *para*-positions (H5, H6).

The results of the ^1H NMR investigation are also in good agreement with the elemental analyses of the compounds. Table 1 shows the experimental and calculated CHN values of the products using a reaction time of 38, 98 and 638 min. It should be noted that after washing no water molecules are enclosed in the framework. In addition, the methylation of the amino groups is also clearly demonstrated by the appearance of new vibrational bands in the IR spectra that are associated with the formation of the methylamine functionality (Fig. 6).

The two possible bands due the symmetric and asymmetric stretching vibration of the amino group (ν N-H) at 3520 and 3390 cm^{-1} are clearly visible in the spectra collected for short reaction times (15, 38 min). The N-H double band vanishes and one broad band at 3393 cm^{-1} due to the N-H vibration of the methylamine is observed for the reactions using a longer reaction time. A new signal at 1285 cm^{-1} is observed, which increases at longer reaction times and can be assigned to the C $_{\text{ar}}$ -N stretching vibration of the methylamine group.³⁰ At the same time, the bands due to the C $_{\text{ar}}$ -N (NH $_2$) vibration at 1260 and 1340 cm^{-1} appear with much lower intensities. This indicates the high degree of methylation of the NH $_2$ groups at longer reaction times.

The IR spectra confirm the results of the ^1H NMR spectroscopy that methylation increases at longer reaction times.

3.4 Influence of the reaction time on the degree of methylation at the reaction temperature of 145 °C

To speed up the crystallisation of CAU-1, the reaction temperature was raised to 145 °C. MW-assisted synthesis was stopped after shorter reaction times (2, 3, 5, and 10 min) in order to minimize the degree of methylation. For the NMR measurements the product was directly dissolved in NaOD/D $_2\text{O}$, which allows detecting the methoxy groups. The ^1H NMR spectra of the washed products show at longer reaction times an increase in the degree of methylation of the amino groups, as well as the increase of the amount of methoxy groups (2.64 ppm, Fig. S4†). This signal can be assigned to CH $_3\text{OD}$, which is formed by the release of the incorporated methoxy groups from the Al-based brick of the CAU-1 framework. According to the composition [Al $_4(\text{OH})_2(\text{OCH}_3)_4(\text{BDC-NH}_2)_3$] for CAU-1-NH $_2$ an integral ratio of methoxy H-atoms to aromatic H-atoms = 4 : 3 (= 1.33)

Table 1 Elemental analysis results of CAU-1 synthesised *via* MW-assisted heating at 135 °C for 38, 98 and 638 min. Calculated values correspond to a composition according to $[Al_4(OH)_2(OCH_3)_4(BDC-NH_{2-x}C_xH_{3x})_3]$

Reaction time/min	Degree of methylation (x) (%)	C_{exp} (calc.) (%)	H_{exp} (calc.) (%)	N_{exp} (calc.) (%)
38	16 (0.16)	42.28 (42.21)	3.72 (3.73)	5.09 (5.18)
98	47 (0.47)	42.90 (42.90)	3.92 (3.90)	5.22 (5.10)
638	95 (0.95)	43.31 (43.92)	4.10 (4.15)	4.98 (4.98)

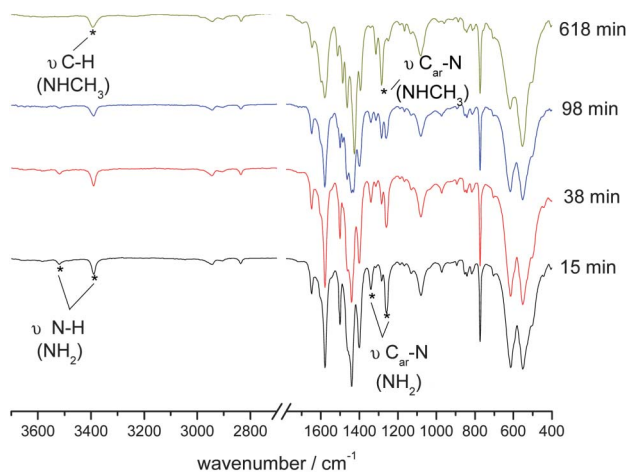


Fig. 6 IR spectra of CAU-1 synthesised *via* MW-assisted heating at the reaction temperature of 135 °C. Four different reaction times were investigated (15, 38, 98 and 638 min).

is expected. Increasing the reaction time from 2 to 10 min leads to integral ratios varying from 1.10 to 1.31, respectively. Thus, short reactions lead only to the partial incorporation of methoxy (83%) groups while after 10 min 99% of the methoxy groups are present. We presume that at very short reaction times structural defects are present. This has also been reported in the synthesis of MOF-5 using short reaction times.³¹

As observed at reaction temperatures of 135 °C, an increase of reaction time leads to a higher degree of methylation of the amino groups, which is clearly visible by an increase of the signal at 2.2 ppm due to the methyl groups. The results are summarized in Table 2.

The lowest degree of methylation of the amino group was found for a reaction time of only two minutes (2%). However, the reaction was not complete and only a very small amount of CAU-1-NH₂ could be obtained (yield < 10% of the washed product, based on aminoterephthalic acid). Using a reaction time

Table 2 Elemental analyses, degree of incorporation of methoxy and methyl groups in CAU-1 synthesised by MW-assisted heating at 145 °C. Reaction times of 2 to 10 min were used. Calculated values are based on a composition according to $[Al_4(OH)_{2+y}(OCH_3)_{4-y}(BDC-NH_{2-x}C_xH_{3x})_3] \cdot wH_2O$

Time/min	Methoxy groups (y) (%)	Degree of methylation (x) (%)	H ₂ O formula (w)	C_{exp} (calc.) (%)	H_{exp} (calc.) (%)	N_{exp} (calc.) (%)
2	83 (0.68)	2 (0.02)	2.3	39.31 (39.34)	3.47 (3.84)	5.34 (5.28)
3	88 (0.48)	3 (0.03)	1.3	40.36 (40.37)	3.53 (3.82)	5.14 (5.12)
5	96 (0.16)	6 (0.06)	—	42.84 (41.84)	3.69 (3.69)	5.34 (5.22)
10	99 (0.04)	13 (0.13)	—	41.81 (42.11)	3.70 (3.71)	5.22 (5.19)

of ten minutes leads to a high yield (90%) but also to a much higher degree of methylation (13%).

The results of the NMR investigation fit well with the elemental analyses of the compounds, which are also listed in Table 2. For the products at reaction times of 2 and 3 min water molecules are enclosed within the framework. The best compromise between the product yield and degree of methylation was determined to be at a reaction time of 3 min. In three repeated reactions the dissolved products exhibit the identical degree of methylation (3%), which clearly shows the good reproducibility of the MW-assisted synthesis (Fig. S5†).

3.5 Influence of the heating method and reactor material

In order to investigate the methylation of the amino groups during the CAU-1 synthesis applying conventional heating methods, reactions were performed in Teflon-lined steel autoclaves and glass autoclaves. A mixture of AlCl₃·6H₂O (463.5 mg, 1.920 mmol) and H₂N-H₂BDC (116.60 mg, 0.645 mmol) was suspended in methanol (6.175 mL) and heated at 125 °C for 5 h. The washed products were directly dissolved in a dilute NaOD/D₂O solution and characterized by ¹H NMR spectroscopy (Fig. 7). Three sets of signals can be observed in the spectra, which can be assigned to aminoterephthalate, *N*-methylaminoterephthalate, and *N,N*-dimethylaminoterephthalate. The signals are discussed for the reaction products obtained in the glass reactor. The labelling of the sets of ¹H signals is listed in Scheme S1† in the ESI. The reaction carried out in a Teflon-lined steel autoclave led to only a small amount of CAU-1-NHCH₃ (12%) compared to the reaction performed in a glass autoclave, which shows that 52% of the amino groups are single methylated and 21.5% of the amino groups are twofold methylated (CAU-1-N(CH₃)₂). The variation of the degree of methylated amino groups as a function of the use of different reaction vessels may be caused by different heating or diffusion rates within the reactors.

3.6 Influence of the thermal activation process on the composition of CAU-1-NH₂

The TG analysis of CAU-1-NH₂ was performed on the degassed sample (30 min/130 °C at 1×10^{-3} bar) in air. The TG curve is shown in Fig. S6†. A very flat step, corresponding to a weight loss of 10%, is observed between 50 and 370 °C. This weight loss cannot be due to the presence of incorporated solvent molecules since this would lead to a well defined step in the TG curve. At higher temperatures, above 370 °C, the decomposition of the frameworks takes place and Al₂O₃ is formed. The observed and calculated total weight loss, based on the final mass of Al₂O₃, fit well (obs. 25.1%, calc. 25.5%). To investigate

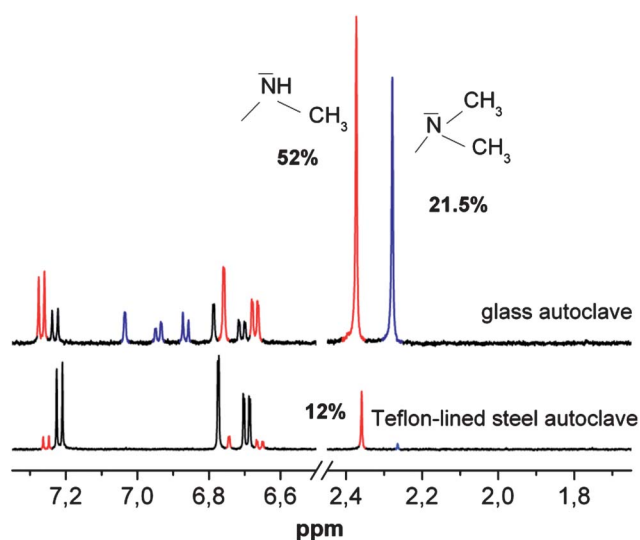


Fig. 7 ^1H NMR spectra of CAU-1 prepared by conventional synthesis using a Teflon-lined autoclave (bottom) or a glass autoclave (top). After the washing process both compounds were directly dissolved in a dilute NaOD/D₂O solution. Each spectrum is normalized to the H3, H6, and H10 signals, respectively. Signals due to the linker molecules are coloured as follows: blue: dimethylated, red: methylated and black: non-methylated.

the processes taking place up to 370 °C the influence of the thermal activation process on the composition of CAU-1-NH₂ was studied using the product obtained by MW-assisted synthesis (3 min/145 °C). In the course of this study different activation times, temperatures and atmospheres (vacuum vs. air) were used. After thermal treatment the samples were characterized by elemental analyses, IR-spectroscopy and ^1H -liquid-state NMR spectroscopy. For the ^1H -liquid-state NMR spectroscopy investigations the samples were directly dissolved in a dilute NaOD/D₂O solution. Elemental analyses and IR spectroscopy were performed on the thermally activated products without any further treatment. Fig. S7† shows the ^1H spectra of the dissolved CAU-1-NH₂ compounds after thermal treatment under different temperatures, activation times, and activation atmospheres (vacuum vs. air). For all five activation procedures, we observed a decrease in the fraction of incorporated methoxy groups retained within the framework (see Table 3). Heating under vacuum at 130 °C for 12 h leads only to the release of a very small fraction of methoxy groups (83% retained) compared to similar heating procedures at 120 °C (55% retained) in air. Even a very short thermal treatment of 30 min at 120 °C leads to a significant removal of methoxy groups (73% retained). While an activation temperature of 190 °C for 12 h leads to an almost complete removal of the incorporated methoxy groups (8% retained), no signal is observed after an activation time of 24 h. Thus methoxy groups are fully replaced by hydroxy groups.

The resulting compound [Al₄(OH)₆(BDC-NH₂)₃] \cdot xH₂O, denoted as CAU-1-NH₂(OH), contains large amounts of adsorbed water molecules, due to a higher hydrophilicity of the framework. Water molecules from the air are necessary for the substitution of methoxy groups by hydroxy groups. This has also been observed previously for thermal activation procedures of acidic zeolite catalysts, which contain surface methoxy

Table 3 Percentage of incorporated methoxy groups within the structure of CAU-1-NH₂, [Al₄(OH)_{2+y}(OCH₃)_{4-y}(BDC-NH_{2-x}C_xH_{3x})₃], after thermal treatment. The CAU-1 products were synthesised by MW-assisted heating using a reaction time of 3 min at 145 °C

Activation procedure	Methoxy groups (%)	Composition in y and x
—	88	$y = 0.48; x = 0.03$
130 °C/12 h (3 mbar)	83	$y = 0.68; x = 0.03$
120 °C/0.5 h	73	$y = 1.08; x = 0.03$
120 °C/12 h	55	$y = 1.80; x = 0.03$
190 °C/12 h	8	$y = 3.68; x = 0.03$
190 °C/24 h	0	$y = 4.00; x = 0.03$
190 °C/12 h (3 mbar)	83	$y = 0.68; x = 0.03$

species.^{32,33} The removal of the methoxy groups is also observed by IR spectroscopy.

The IR spectra of CAU-1-NH₂ before and after the thermal treatment in air (190 °C/24 h) are shown in Fig. 8. The two broad bands due to the symmetric and asymmetric modes of C-H stretching vibration of the bridging methoxy groups at 2940 and 2840 cm⁻¹ and the C-O stretching vibration of the incorporated methoxy groups at ~1080 cm⁻¹ vanish in the spectrum of the heated sample. At the same time, the intensity of the weak signal at ~3700 cm⁻¹ due to the bridging OH groups increases. The powder pattern of the washed sample exhibits no significant change in crystallinity after thermal treatment (see Section 3.8 and Fig. 13).

3.7 Post-synthetic modification of CAU-1-NH₂

Using MW-assisted heating for the syntheses of CAU-1 led to non-methylated amino groups at very short reaction times. This should allow the post-synthetic modification of the amino functionality, which has been previously reported, for example, for Al-MIL-53-NH₂ and IRMOF-3.^{16,34} For the proof of principle we reacted CAU-1-NH₂ with acetic anhydride, which led to the fully acylated compound CAU-1-NHCOCH₃ ([Al₄(OH)₂(OCH₃)₄(BDC-NHCOCH₃)₃] \cdot xH₂O) (Scheme 2).

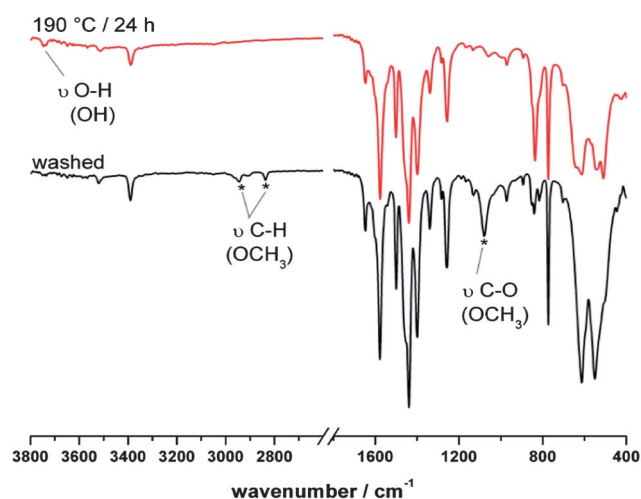
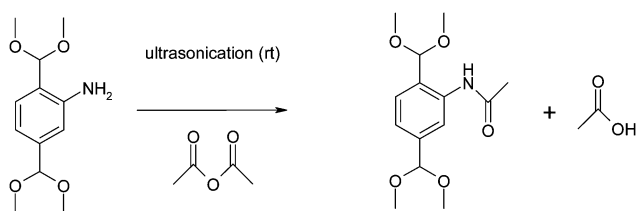


Fig. 8 Comparison of the IR-spectra of washed CAU-1 before (black) and after thermal treatment (190 °C for 24 h in air) (red).



Scheme 2 Post-synthetic modification of CAU-1-NH₂ by reaction with acetic anhydride.

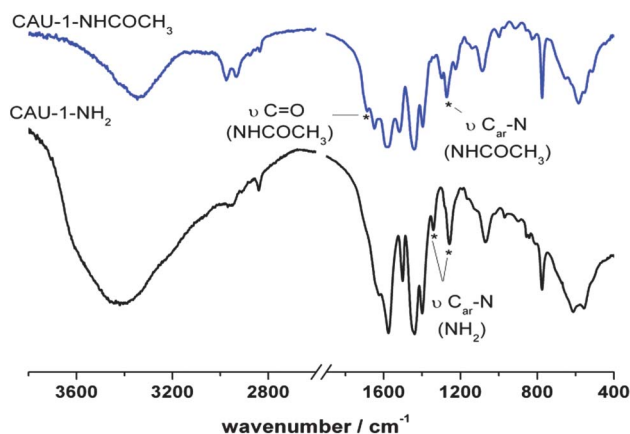


Fig. 9 IR spectra of modified CAU-1 (blue) and unmodified CAU-1-NH₂ (black). The characteristic bands in the spectra are marked with black stars.

Fig. 9 shows the IR spectra of the CAU-1-NH₂ and CAU-1-NHCOCH₃. New signals at 1690 and 1274 cm⁻¹ in the spectrum of CAU-1-NHCOCH₃ are caused by the C=O and the C_{ar}-N stretching vibrations of the amide group respectively.³⁰ At the same time, the bands due to the C_{ar}-N (NH₂) stretching vibration at 1258 and 1341 cm⁻¹ do not appear in the spectrum

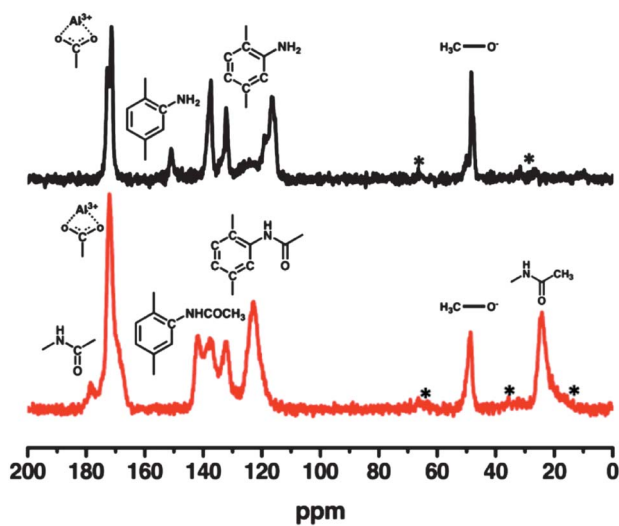


Fig. 10 ¹³C MAS NMR spectra of CAU-1-NH₂ (black) and CAU-1-NHCOCH₃ (red). The signals marked by an asterisk (*) are due to spinning side bands.

anymore. This indicates a nearly complete modification of the NH₂ groups.

The results of the IR-spectroscopic measurements of the post-synthetic modification of CAU-1-NH₂ are also confirmed by solid-state ¹³C and ¹⁵N MAS NMR experiments (Fig. 10 and 11).

In contrast to the material obtained by conventional heating (see Ahnfeldt *et al.*,¹⁷ Fig. S5b†), the ¹³C spectrum of CAU-1-NH₂ shows no signal at 27 ppm (Fig. 10, top). This depicts that there are no -NHCH₃ groups present. Upon post-synthetic modification, two new signals at 24 ppm and 178 ppm are observed, which can be assigned to the methyl group of the acetamide and the carbonyl ¹³C atom, respectively. The signal of the ipso carbon atom, which is closest to the newly formed amide bond, shifts from 150 ppm to 141 ppm.

The ¹⁵N CPMAS-NMR spectrum of CAU-1-NH₂ (Fig. 11) exhibits a signal at -316 ppm, which we assigned to the -NH₂ group. The signal due to the N-atom of the amino group shifts in the spectrum of CAU-1-NHCOCH₃ to -253 ppm caused by the formation of the amide group. There is no signal left at -316 ppm which confirms a complete modification of the -NH₂ group.

Further structural information for CAU-1-NHCOCH₃ could be gained by a series of solid-state NMR experiments like ¹H-¹H spin diffusion spectra and carbon-proton HETCOR spectra. In Fig. 12 different ¹H spin diffusion spectra of CAU-1-NHCOCH₃ as a function of the mixing times are shown. The signal assignment for these spectra is as follows: at 0.8 and 1.5 ppm two signals for the methyl protons of the acetyl residue, at 3.0 ppm a signal for the methoxy groups, at 7-8 ppm a broad signal for the aromatic protons and at 9 ppm the NH proton signal.

For very short spin diffusion mixing times (1 μs) no correlation occurs, at short mixing times (700 μs) first spatial proximity can be observed between the signal at 3.0 ppm and 1.5 ppm which we assign to the methoxy groups of the inorganic brick and the methyl group of the acetamide, respectively. This can only be explained by a short distance between the methoxy groups and a part of the linker residues. At medium mixing times (1500 μs) the other correlations begin to develop, whereas even at longer mixing times (4000 μs) the correlation between the signal

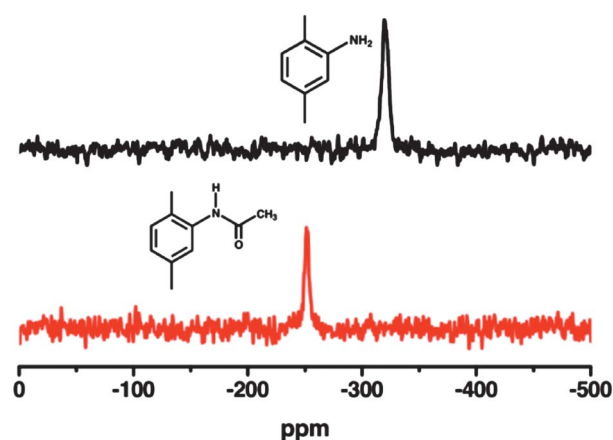


Fig. 11 ¹⁵N CPMAS NMR spectra of CAU-1-NH₂ (black) and CAU-1-NHCOCH₃ (red).

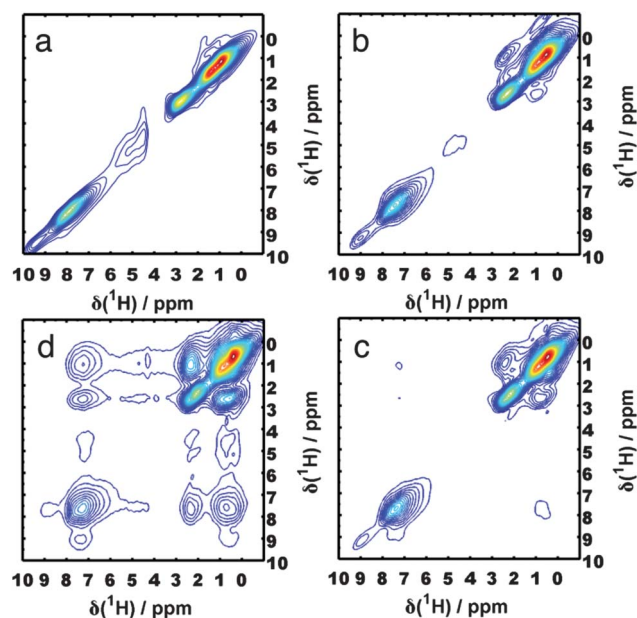


Fig. 12 2D spin diffusion spectra of CAU-1-NHCOCH₃ at mixing times of 1 μ s (a), 700 μ s (b), 1500 μ s (c) and 4000 μ s (d).

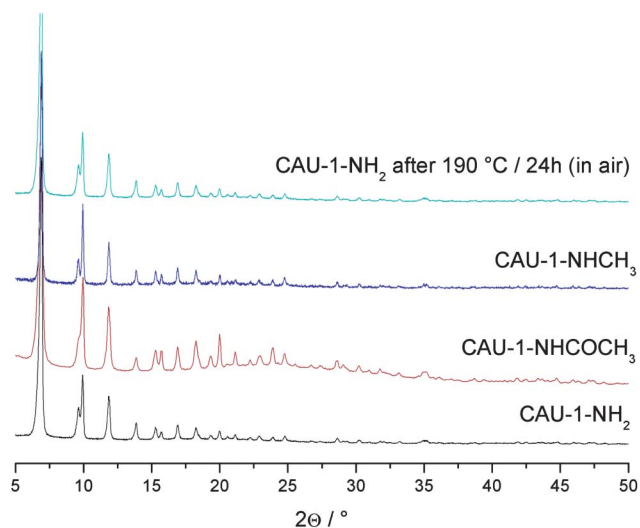


Fig. 13 XRPD patterns of CAU-1-NH₂ (black), CAU-1-NHCOCH₃ (red), CAU-1-NHCH₃ (blue), and CAU-1-NH₂ after thermal treatment at 190 °C for 24 h in air (green).

Table 4 Refined lattice parameters determined from XRPD data of CAU-1-X (X = -NH₂, -NHCH₃, -NHCOCH₃) and CAU-1-NH₂(OH), which was heated before the measurement to exchange the incorporated methoxy groups by hydroxy groups (190 °C/24 h in air)

Compound	<i>a</i> /Å	<i>b</i> /Å	<i>c</i> /Å	<i>V</i> /Å ³
CAU-1-NH ₂	18.319(4)	18.319(4)	17.753(7)	5958(1)
CAU-1-NHCH ₃	18.331(5)	18.331(5)	17.739(7)	5960(2)
CAU-1-NHCOCH ₃	18.341(5)	18.341(5)	17.735(4)	5966(1)
CAU-1-NH ₂ (OH)	18.330(6)	18.330(6)	17.761(7)	5968(1)

at 3.0 and 0.8 ppm is still weak. We interpret this behaviour as a long distance between methoxy groups and methyl groups of these linker residues. This is only possible if there are different positions for the methyl residues available, like an orientation dependence between an alignment of the linker into the smaller pores (short distances) and into the bigger pores (longer distances). For this model we estimate *via* the intensity ratio of the signals at 1.5 and 0.8 ppm one-third of the linker molecules to be oriented into the small pores and two-thirds into the bigger pores as a possible scenario.

Similar experiments were conducted for CAU-1-NHCH₃, but no such behaviour could be observed (see Fig. S1†). This could be explained by the smaller volume of the methyl residues relative to the acetyl residue of CAU-1-NHCOCH₃.

3.8 XRPD studies on CAU-1-NH₂, CAU-1-NHCH₃, CAU-1-NHCOCH₃ and CAU-1-NH₂(OH)

CAU-1-NH₂, CAU-1-NHCH₃, and CAU-1-NHCOCH₃ could be synthesized with high crystallinity and without crystalline impurities. The thermal treatment of CAU-1-NH₂ at 190 °C for 24 h in air led to a complete replacement of the methoxy by the hydroxy groups. Fig. 13 shows powder patterns of all three products, as well as the one of CAU-1-NH₂ after thermal treatment (190 °C/24 h in air).

To determine the influence of the composition on the crystal structure, the lattice parameters were determined by using WinXPow.²⁸ Lattice parameter refinements and systematic extinctions led for all compounds to a tetragonal body-centred unit cell with very similar lattice parameters in all four cases (Table 4).

3.9 Temperature-dependent X-ray powder diffraction measurement (TD-XRPD)

For investigating the influence of the different compositions of the compounds on the thermal properties TD-XRPD measurements of all four compounds were performed. The TD-XRPD measurements of CAU-1-NH₂, CAU-1-NH₂(OH), CAU-1-NHCH₃ and CAU-1-NHCOCH₃ are shown in Fig. 14 and S8–S10†, respectively. In good agreement with the results of the TG analysis of CAU-1-NH₂ (Fig. S6†), all investigated

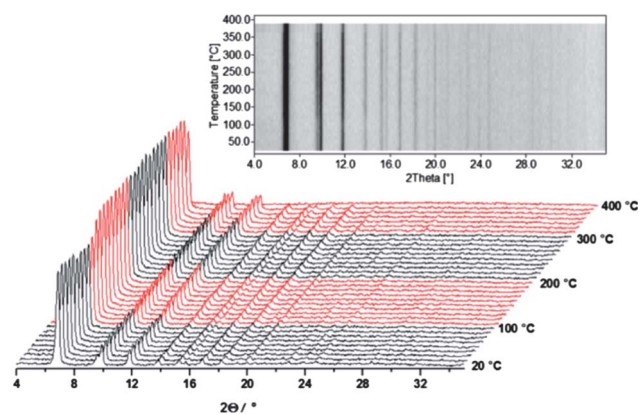


Fig. 14 Temperature-dependent X-ray powder diffraction patterns of CAU-1-NH₂ in air (20–400 °C).

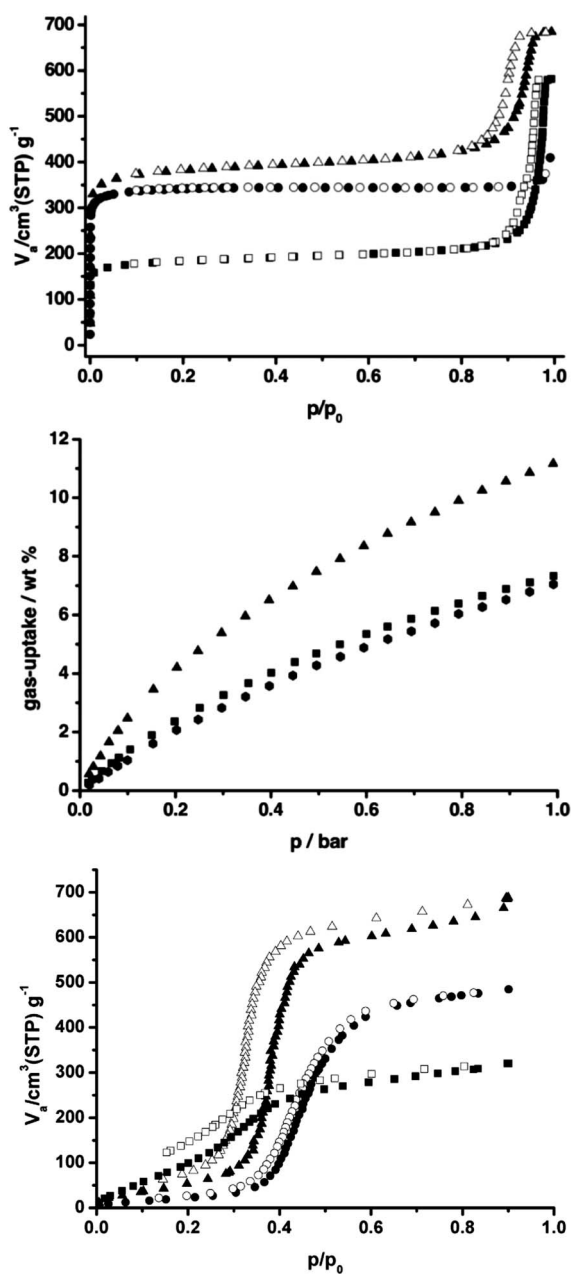


Fig. 15 N_2 (top), CO_2 (middle) and H_2O (bottom) sorption isotherms for CAU-1- NH_2 (\bullet = adsorption, \circ = desorption), CAU-1- $NHCH_3$ (\blacktriangle = adsorption, \triangle = desorption) and CAU-1- $NHCOCH_3$ (\blacksquare = adsorption, \square = desorption). The H_2O and CO_2 sorption isotherms were collected at 298 K, N_2 sorption experiments at 77 K.

compounds show a high thermal stability at least up to 350 °C. At around 100 °C, increased reflection intensities were observed in the TD-XRPD measurements, which are accompanied by the removal of absorbed water molecules. Up to the decomposition of the framework, no changes of the reflection positions are detectable.

However, a comparison of the TD-XRPD measurement of all four CAU-1 derivatives led to the conclusion that the different compositions have no or only a minor influence on their thermal behaviour.

Table 5 Comparison of specific surface area S_A , total pore volume $V(N_2)$ and total pore volume $V(H_2O)$ of CAU-1- NH_2 , CAU-1- $NHCH_3$, and CAU-1- $NHCOCH_3$

CAU-1-X	- NH_2	- $NHCH_3$	- $NHCOCH_3$
$S_A/m^2 g^{-1}$	1530	1340	680
$V(N_2)^a/cm^3 g^{-1}$	0.64	0.53	0.30
$V(H_2O)^b/cm^3 g^{-1}$	0.55	0.48	0.25
wt CO_2^c (%)	11.2	7.0	7.3

^a Calculated at $p/p_0 = 0.5$ from the nitrogen adsorption isotherm and 77 K. ^b Calculated at $p/p_0 = 0.9$ from the water adsorption isotherm and 298 K. ^c Calculated at 1 bar and 298 K.

3.10 Sorption study on CAU-1

The three CAU-1 derivatives, CAU-1- NH_2 , CAU-1- $NHCH_3$, and CAU-1- $NHCOCH_3$, show different sorption properties depending on the functional group and the adsorbate employed (Fig. 15).

Using nitrogen (Fig. 15, top), Type 1 isotherms are observed for all three compounds. The apparent specific surface area, calculated using the BET equation, decreases strongly from 1530 $m^2 g^{-1}$ (CAU-1- NH_2) to 680 $m^2 g^{-1}$ (CAU-1- $NHCOCH_3$) depending on the size of the functional group. Accordingly, the micropore volume also decreases from 0.64 $cm^3 g^{-1}$ (CAU-1- NH_2) to 0.30 $cm^3 g^{-1}$ (CAU-1- $NHCOCH_3$). Adsorption experiments with water vapour show a higher uptake for CAU-1- $NHCOCH_3$ at low p/p_0 values compared to CAU-1- NH_2 and CAU-1- $NHCH_3$. This may be due to hydrogen bonding interactions of the amide group, which decrease in the order $-NHCOCH_3 > -NH_2 > -NHCH_3$, as well as a higher adsorption potential due to narrower pore sizes. The order is in agreement with the desorption curves of CAU-1- $NHCOCH_3$ and CAU-1- NH_2 , where a slight hysteresis due to these stronger interactions with the adsorbate is observed. The micropore volume calculated from the water adsorption isotherms (Fig. 15, bottom) is smaller than the calculated micropore volume from the nitrogen isotherms, as observed for other MOFs like DUT-4 and HKUST-1.³⁵ The CO_2 sorption measurements of the three compounds (Fig. 15, middle) were carried out at 298 K and up to 1 bar. Under this condition, the maximum uptake was not accomplished. However, the isotherm of CAU-1- NH_2 shows a higher uptake of CO_2 (11.2 wt%) than the isotherms of CAU-1- $NHCOCH_3$ (7.3 wt%) and CAU-1- $NHCH_3$ (7.0 wt%). The higher uptake of CO_2 from the amide functionalized CAU-1 compared to CAU-1- $NHCH_3$ could be explained by stronger host-guest interactions of the adsorbent with CO_2 . The results of all sorption measurements are summarised in Table 5.

4. Conclusion

In summary, we have demonstrated that in the field of porous materials the presence of guest molecules, like solvent or uncoordinated linker molecules, can easily result in a misinterpretation of the data. Thus, an extensive characterisation of the reaction products of MOF syntheses is mandatory to fully understand structure-property relationships.

In the case of CAU-1, X-ray diffraction, IR- as well as liquid-state and solid-state NMR-spectroscopy, *in situ* EDXRD,

TD-XRPD, thermogravimetric and elemental analysis, sorption experiments and dynamic light scattering have been applied. Surprisingly, not only the synthesis conditions during the product formation lead to isorecticular products of different compositions, *i.e.*, variation of the degree of methylation, but also the activation procedure needs to be controlled in detail.

We showed the various modifications of the organic linker. By conventional heating methylation of the amino residue occurs depending on the reaction time, whereas by MW-assisted synthesis and short reaction times methylation can be suppressed completely. Even post-synthesis modification is possible *via* acetylation of the amino group.

Also the modification of the inorganic brick is possible during the activation process in air *via* substitution of the methoxy by hydroxy groups.

Liquid- and solid-state NMR spectroscopy proved to be an essential tool for the thorough investigation of the synthesis routes. *Via* solid-state NMR spectroscopy the methylation reaction under conventional synthesis conditions was discovered and the post-synthetic modification as well as the linker orientation were studied.

Acknowledgements

The authors thank Michael Wharmby for cross-reading this article and fruitful discussions. The state of Schleswig-Holstein and the Deutsche Forschungsgemeinschaft (DFG, SPP 1362) "Porous Metal–Organic Frameworks" under the grant STO 643/5-2 and SE 1417/3-2 are gratefully acknowledged for the financial support. The research leading to these results has received funding from the European Community's Seventh Framework Programme (FP7/2007-2013) under grant agreement no. 228862.

Notes and references

- 1 U. Mueller, M. Schubert, F. Teich, H. Puetter, K. Schierle-Arndt and J. Pastre, *J. Mater. Chem.*, 2006, **16**, 626.
- 2 P. Horcajada, C. Serre, M. Vallet-Reg, M. Sebban, F. Taulelle and G. Férey, *Angew. Chem., Int. Ed.*, 2006, **45**, 5974.
- 3 J. Li, R. Kuppler and H. Zhou, *Chem. Soc. Rev.*, 2009, **38**, 1477.
- 4 J. Y. Lee, O. K. Farha, J. Roberts, K. A. Scheidt, S. T. Nguyen and J. T. Hupp, *Chem. Soc. Rev.*, 2009, **38**, 1450.
- 5 G. Lu and J. T. Hupp, *J. Am. Chem. Soc.*, 2010, **132**, 7832.
- 6 M. Gaab, N. Trukhan, S. Maurer, R. Gummaraju and U. Müller, *Microporous Mesoporous Mater.*, 2011, DOI: 10.1016/j.micromeso.2011.08.016.
- 7 (a) H. Reinsch, M. Krüger, J. Wack, J. Senker, F. Salles, G. Maurin and N. Stock, *Microporous Mesoporous Mater.* DOI: 10.1016/j.micromeso.2011.05.029; (b) C. Volkringer, T. Loiseau, M. Haouas, F. Taulelle, D. Popov, M. Burghammer, C. Riekel, C. Zlotea, F. Cuevas, M. Latroche, D. Phanon, C. Knöfelv, P. L. Llewellyn and G. Férey, *Chem. Mater.*, 2009, **21**, 5783; (c) A. Comotti, S. Bracco, P. Sozzani, S. Horike, R. Matsuda, J. Chen, M. Takata, Y. Kubota and S. Kitagawa, *J. Am. Chem. Soc.*, 2008, **130**, 13664.

- 8 C. Volkringer, T. Loiseau, N. Guillou, G. Férey, M. Haouas, F. Taulelle, N. Audebrand, I. Margiolaki, D. Popov, M. Burghammer and C. Riekel, *Cryst. Growth Des.*, 2009, **9**, 2927.
- 9 T. Loiseau, C. Serre, C. Huguenard, G. Fink, F. Taulelle, M. Henry, T. Bataille and G. Férey, *Chem.–Eur. J.*, 2004, **10**, 1373.
- 10 (a) T. Loiseau, C. Mellot-Draznieks, H. Muguerra, G. Férey, M. Haouas and F. Taulelle, *C. R. Chim.*, 2005, **8**, 765; (b) I. Senkowska, F. Hoffmann, M. Fröba, J. Getzschmann, W. Böhlmann and S. Kaskel, *Microporous Mesoporous Mater.*, 2009, **122**, 93.
- 11 (a) T. Loiseau, L. Lecroq, C. Volkringer, J. Marrot, G. Férey, M. Haouas, F. Taulelle, S. Bourrelly, P. L. Llewellyn and M. Latroche, *J. Am. Chem. Soc.*, 2006, **128**, 10223; (b) C. Volkringer, D. Popov, T. Loiseau, G. Férey, M. Burghammer, C. Riekel, M. Haouas and F. Taulelle, *Chem. Mater.*, 2009, **21**, 5695.
- 12 (a) T. Ahnfeldt, J. Moellmer, V. Guillerm, R. Staudt, C. Serre and N. Stock, *Chem.–Eur. J.*, 2011, **23**, 6462; (b) S. Biswas, T. Ahnfeldt and N. Stock, *Inorg. Chem.*, 2011, **50**, 9518; (c) D. Himsl, D. Wallacher and M. Hartmann, *Angew. Chem., Int. Ed.*, 2009, **48**, 4639.
- 13 A. Boutina, S. Couck, F.-X. Coudert, P. Serra-Crespo, J. Gascon, F. Kapteijn, A. H. Fuchs and J. F. M. Denayer, *Microporous Mesoporous Mater.*, 2011, **140**, 108.
- 14 P. Serra-Crespo, E. V. Ramos-Fernandez, J. Gascon and F. Kapteijn, *Chem. Commun.*, 2011, **47**, 8578.
- 15 K. K. Tanabe and S. M. Cohen, *Chem. Soc. Rev.*, 2011, **40**, 498.
- 16 (a) T. Ahnfeldt, D. Gunzelmann, T. Loiseau, D. Hirsemann, J. Senker, G. Férey and N. Stock, *Inorg. Chem.*, 2009, **48**, 3057; (b) J. Gascon, U. Aktay, M. D. Hernandez-Alonso, G. P. M. van Klink and F. Kapteijn, *J. Catal.*, 2009, **261**, 75.
- 17 T. Ahnfeldt, N. Guillou, D. Gunzelmann, I. Margiolaki, T. Loiseau, G. Férey, J. Senker and N. Stock, *Angew. Chem., Int. Ed.*, 2009, **48**, 5163.
- 18 P. Serra-Crespo, E. V. Ramos-Fernandez, J. Gascon and F. Kapteijn, *Chem. Mater.*, 2011, **23**, 2565.
- 19 Comment: CAU-1 refers to the general framework structure of these compounds. In the following the functionalisation of the $-NH_2$ groups ($-NH_2$, $NHCH_3$, $-N(CH_3)_2$) is explicitly stated to prevent further confusion.
- 20 J. H. Cavka, S. Jakobsen, U. Olsbye, N. Guillou, C. Lamberti, S. Bordiga and K. P. Lillerud, *J. Am. Chem. Soc.*, 2008, **130**, 13850.
- 21 M. Dan-Hardi, C. Serre, T. Frot, L. Rozes, G. Maurin, C. Sanchez and G. Férey, *J. Am. Chem. Soc.*, 2009, **131**, 10857.
- 22 F. Hinterholzinger, C. Scherb, T. Ahnfeldt, N. Stock and T. Bein, *Phys. Chem. Chem. Phys.*, 2010, **12**, 4515.
- 23 X. Si, C. Jiao, F. Li, J. Zhang, S. Wang, S. Liu, Z. Li, L. Sun, F. Xu, Z. Gabelica and C. Schick, *Energy Environ. Sci.*, 2011, **4**, 4522.
- 24 M. Pera-Titus, M. Savonnet and D. Farrusseng, *J. Phys. Chem. C*, 2010, **114**, 17665.
- 25 M. Savonnet, E. Kockrick, A. Camarata, D. Bazer-Bachi, N. Bats, V. Lecocq, C. Pinela and D. Farrusseng, *New J. Chem.*, 2011, **35**, 1892.
- 26 T. Ahnfeldt and N. Stock, *CrystEngComm*, 2012, **14**, 505.
- 27 A. Boulitif and D. Louer, *J. Appl. Crystallogr.*, 1991, **24**, 987.
- 28 *STOE WinXPOW version 2.11*, Stoe & Cie GmbH, Darmstadt, Germany, 2005.
- 29 A. Lesage and L. Emsley, *J. Magn. Reson.*, 2001, **148**, 449.
- 30 G. Socrates, *Infrared and Raman Characteristic Group Frequencies: Tables and Charts*, Wiley & Sons, West Sussex, UK, 3rd edn, 2004.
- 31 U. Ravon, M. Savonnet, S. Aguado, M. E. Domine, E. Janneau and D. Farrusseng, *Microporous Mesoporous Mater.*, 2010, **129**, 319.
- 32 W. Wang, A. Buchholz, M. Seiler and M. Hunger, *J. Am. Chem. Soc.*, 2003, **125**, 15260.
- 33 W. Wang and M. Hunger, *Acc. Chem. Res.*, 2008, **41**, 895.
- 34 Z. Wang and S. M. Cohen, *J. Am. Chem. Soc.*, 2007, **129**, 12368.
- 35 P. Küsgens, M. Rose, I. Senkowska, H. Fröde, A. Henschel, S. Siegle and S. Kaskel, *Microporous Mesoporous Mater.*, 2009, **120**, 325.